EPJ Web of Conferences **164**, 07015 (2017) DOI: 10.1051/epjconf/201716407015
ICNFP 2016

Forward-backward multiplicity correlations in proton-proton collisions from several GeV to LHC energies

L. Bravina[1,a], J. Bleibel[2,3], R. Emaus[1], and E. Zabrodin[1,4,5]

[1] *Department of Physics, University of Oslo, PB 1048 Blindern, N-0316 Oslo, Norway*
[2] *Max-Planck-Institut für Intelligente Systeme, Heisenbergstr. 3, D-70569 Stuttgart, Germany*
[3] *Institut für Augewandte Physik, Universität Tübingen, Auf der Morgenstelle 10, D-72076 Tübingen, Germany*
[4] *Skobeltsyn Institute of Nuclear Physics, Moscow State University, RU-119991 Moscow, Russia*
[5] *National Research Nuclear University "MEPhI" (Moscow Engineering Physics Institute), Kashirskoe highway 31, Moscow, RU-115409, Russia*

Abstract. Forward-backward multiplicity correlations in pp collisions at LHC energies are studied with the quark-gluon string model. Comparison with experimental data and with model calculations for lower energies is performed. The model correctly reproduces the linear slope of the correlations, $\langle n_B(n_F)\rangle = a + b_{corr}n_F$, in the whole energy interval. Positive correlations arise because of mixing of sub-processes with different mean multiplicities. The increase of b_{corr} with rising collision energy is linked to the increase of the variety of sub-processes going via the soft and hard multi-Pomeron exchanges. For the events with fixed amount of Pomerons the correlation slope b_{corr} is shown to be essentially zero.

1 Introduction

The first observation of significant positive correlations between the multiplicity of charged particles emitted in forward and backward hemispheres in $\bar{p}p$ collisions at ISR energies was considered as evidence of long range correlations between the "clusters" of fragmenting system [1]. This phenomenon has attracted a lot of attention, see e.g. [2–8] and references therein. Positive forward-backward (FB) correlations in multiplicity were found in hadronic interactions at energies from several GeV to $\sqrt{s}$ = 1.8 TeV [9–12]. In contrast, no significant FB correlations were observed in e^+e^- annihilation at energies up to $\sqrt{s}$ = 93 GeV [13] and 133 GeV [14].

It appeared soon that the FB multiplicity correlations possessed the following properties:

- the linear dependence of the averaged multiplicity of charged particles emitted in forward (or backward) hemisphere on the multiplicity of charged particles emitted in the opposite hemisphere, i.e.,

$$\langle n_B(n_F)\rangle = a + b_{corr}n_F \ . \tag{1}$$

[a] e-mail: larissa.bravina@fys.uio.no

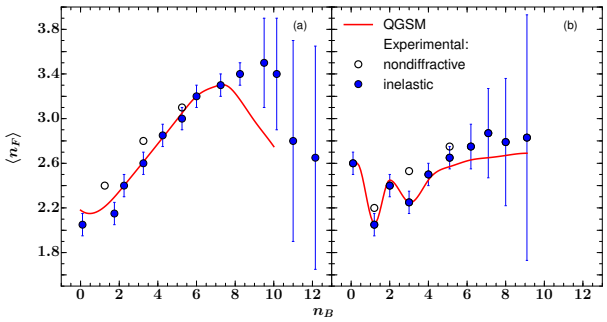

Figure 1. (a): Dependence $\langle n_F \rangle (n_B)$ of charged particles in inelastic (solid circles) and nondiffractive (open circles) $\bar{p}p$ collisions at 32 GeV/c. Solid curve denotes the QGSM calculations. **(b)**: The same as **(a)** but for pp interactions at 32 GeV/c.

The slope parameter b_{corr} is defined as

$$b_{corr} = \frac{\langle (n_F - \langle n_F \rangle)(n_B - \langle n_B \rangle) \rangle}{\left[\langle (n_F - \langle n_F \rangle)^2 \rangle \langle (n_B - \langle n_B \rangle)^2 \rangle \right]^{1/2}} , \quad (2)$$

where n_F and n_B represent multiplicities of charged particles in forward and backward hemispheres, respectively.

- the correlations reveal positive slope b_{corr} for particles from the central region $|x_F| < 0.1$, whereas for particles from the fragmentation regions $|x_F| > 0.1$ the slope is consistent with zero

- the strength of the correlations increases with rising collision energy

- for events with very high particle multiplicity the correlation strength is weakened.

On a phenomenological level these features were explained by mixture of emitting clusters with different mean multiplicity [4]. To provide a linear dependence given by Eq. (1) the clusters should obey the Poisson distribution [8].

We would like to present here our study of forward-backward multiplicity correlations within the quark-gluon string model (QGSM) [15] and its Monte Carlo version [16, 17]. The details of the model can be found in these Proceedings in [18]. QGSM was successfully applied for the description of FB correlations in pp and $\bar{p}p$ collisions at $p_{lab} = 32$ GeV/c [10], and recently in pp collisions at LHC energies 900 GeV $\leq \sqrt{s} \leq$ 13 TeV [19]. Results of the both studies are presented below.

2 FB correlations in pp and $\bar{p}p$ interactions at intermediate energies

In [10] the FB multiplicity correlations were studied in both pp and $\bar{p}p$ collisions at $p_{lab} = 32$ GeV/c. The experiments were carried out on the big bubble chamber “Mirabelle" (ITEP, Serpukhov). Figure 1 shows the $\langle n_F \rangle (n_B)$ dependence of charged particles measured in inelastic and in nondiffractive pp and $\bar{p}p$ interactions. Calculations of QGSM are plotted onto the experimental results as well. The model correctly reproduces the data. One can see that the slope b_{corr} of the distributions in $\bar{p}p$ collisions is steeper than that in pp collisions. For both reactions, the FB multiplicity correlations seem to be stronger in inelastic collisions compared to non-single diffractive (NSD) ones.

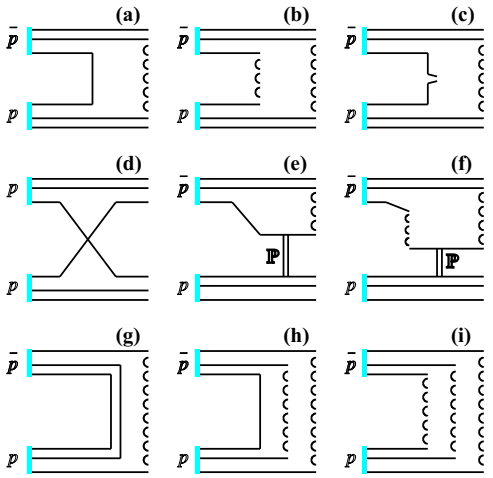

Figure 2. Diagrams taken into account in QGSM in the modeling of $\bar{p}p$ and pp interactions at intermediate energies: (a) planar, (b) cylinder, (c) undeveloped cylinder, (d) binary, (e)-(f) single diffraction with low-mass and high-mass excitation, (g)-(j) annihilation diagrams.

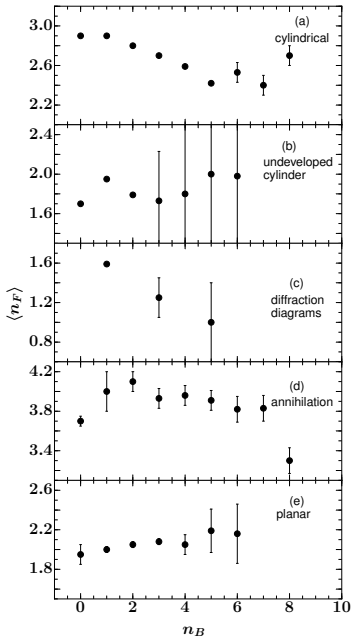

Figure 3. Dependencies $\langle n_F \rangle(n_B)$ for individual mechanisms of $\bar{p}p$ interactions at 32 GeV/c in the QGSM: cylinder diagrams (a), undeveloped cylinder diagrams (b), diffraction diagrams (c), annihilation diagrams (d), and planar diagrams (e).

Table 1. Slope parameters b_{corr} of the forward-backward correlations in inelastic and NSD pp and $\bar{p}p$ collisions at 32 GeV/c.

Reaction	pp	$\bar{p}p$
non-single diffraction	0.070±0.009	0.177±0.010
inelastic	0.098±0.006	0.192±0.007
inelastic, $\|x_F\| < 0.1$	0.237±0.007	0.175±0.006
inelastic, $\|x_F\| > 0.1$	0.013±0.006	-0.073±0.006

To present this more distinctly, we list the slope parameters in Table 1 for inelastic and NSD events. The data were also extracted for central ($|x_F| < 0.1$) and for non-central ($|x_F| > 0.1$) regions in inelastic collisions. The positive FB correlations are observed for central region $|x_F| < 0.1$ only, whereas for the regions with $|x_F| > 0.1$ there are practically no correlations.

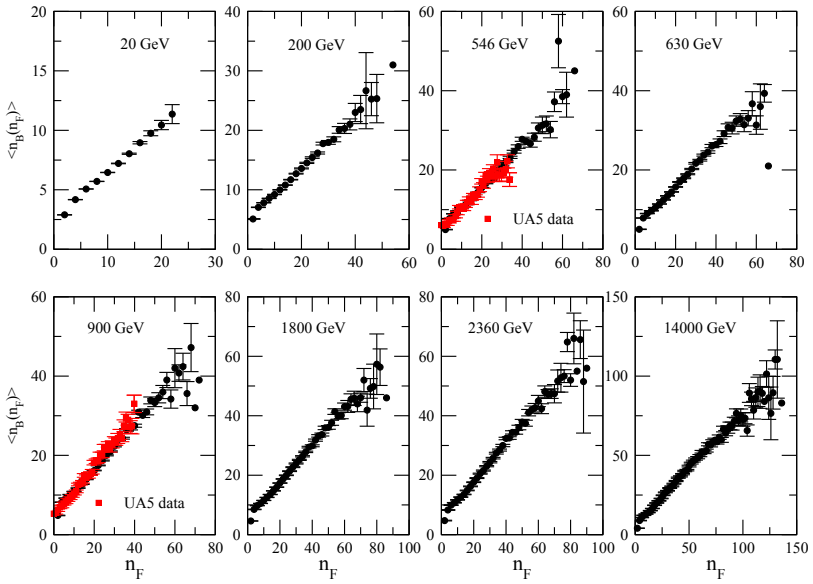

Figure 4. Dependencies $\langle n_B \rangle (n_F)$ for rapidity interval $0 \leq \eta \leq 4$ in NSD pp collisions at 20 GeV$\leq \sqrt{s} \leq$ 14 TeV. Data for 546 GeV and 900 GeV (from [3]) are shown by full squares.

For better understanding of the reason why the FB correlations in $\bar{p}p$ collisions are stronger at this energy than the FB correlations in pp collisions, we plot in Fig. 2 the set of diagrams employed in QGSM for treatment of both types of collisions at intermediate energies. Obviously, the variety of sub-processes in $\bar{p}p$ interactions is richer compared to that in pp ones, because, e.g., the planar diagrams (a) and annihilation diagrams (g)-(i) are absent in pp processes. Since more sub-processes with different mean multiplicities contribute to particle production in $\bar{p}p$ collisions, the correlation slope is steeper, i.e. $b_{corr}^{\bar{p}p} > b_{corr}^{pp}$. Similarly, because of the lack of single diffraction diagrams the correlation strength in non-single diffractive (NSD) processes is smaller compared to that in inelastic ones. Figure 3 displays the FB correlations for different sub-processes shown in Fig. 2, namely, cylinder diagram, undeveloped cylinder, single diffraction, $\bar{p}p$ annihilation and planar diagram. Only the planar sub-processes demonstrate weak positive FB correlations, whereas the correlation slopes for cylinder and diffractive diagrams are slightly negative.

The cross section of annihilation process drops rapidly with rising energy of the collisions. Therefore, the slopes of FB multiplicity correlations in pp and $\bar{p}p$ interactions become similar after some collision energy threshold. The strength of the correlations continues to increase, as shown in Fig. 4. Here QGSM calculations of FB correlations in pp interactions are displayed for energies ranging from $\sqrt{s}$ = 20 GeV to $\sqrt{s}$ = 14 TeV. Comparison with the UA5 data on $\bar{p}p$ collisions at $\sqrt{s}$ = 546 GeV and 900 GeV [3, 11] demonstrates a good agreement between the model calculations and the experimental data. For all reactions the slope of the FB correlations remains almost linear. We have mentioned already the vanishing of annihilation diagrams, as well as other so-called pre-asymptotic diagrams, with the increase of collision energy. However, the only reason of enlargement of the correlation strength b_{corr} in the model is the rise of the variety of different sub-processes with different mean multiplic-

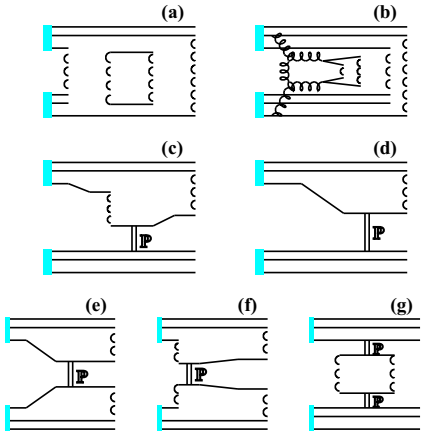

Figure 5. Diagrams taken into account in QGSM in the modeling of pp interactions at ultrarelativistic energies: (a) multi-Pomeron exchange, (b) (semi)hard gluon-gluon interaction and soft Pomeron exchange, (c)-(d) single diffraction with high-mass and low-mass excitation, (e)-(f) double diffraction with low-mass and high-mass excitation, (g) central diffraction.

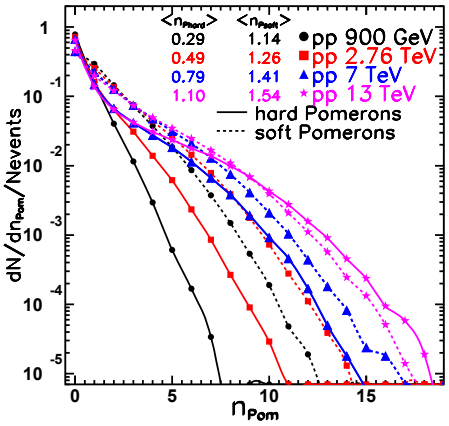

Figure 6. Average numbers of soft (dotted curves) and hard (solid curves) Pomerons per event in pp collisions at $\sqrt{s}$ = 0.9, 2.76, 7, and 13 TeV, respectively.

ity. These sub-processes and their role in formation of FB multiplicity correlations at ultra-relativistic energies are discussed in 3.

3 FB correlations at LHC energies

The set of diagrams describing the pp interactions at ultra-relativistic energies is shown in Fig.5. The first two diagrams represent (a) the soft (multi)Pomeron exchanges and (b) processes going via the formation of hard Pomerons. Other diagrams deal with the processes of single diffraction, (c) and (d), and double diffraction, (e)-(g). The main contribution to particle multiplicity comes from the processes with soft and hard Pomeron exchanges. Their numbers increase with rising collision energy, as it can be seen in Fig. 6. This figure displays the relative amounts of soft and hard Pomerons in a single pp-event at energies $\sqrt{s}$ = 900 GeV, 2.76 TeV, 7 TeV and 13 TeV, respectively. At $\sqrt{s}$ = 900 GeV the number of soft Pomerons exceeds the number of hard Pomerons by factor 4, whereas at $\sqrt{s}$ = 13 TeV their ratio drops to 1.4. As it follows from Fig. 6, the maximum number of both soft and hard Pomerons in a single event gradually increases with collision energy. The variety of sub-processes containing all possible combinations of soft and hard Pomerons becomes more extensive. Since these processes have different mean multiplicities of produced hadrons, the strength of the FB correlations measured for the whole sample of events increases, as shown in Fig. 7. One can see that the FB correlations are not very strong at low multiplicity area, $n^{ch} \leq 15$. The slopes of the distributions are also becoming less steep after a certain multiplicity threshold.

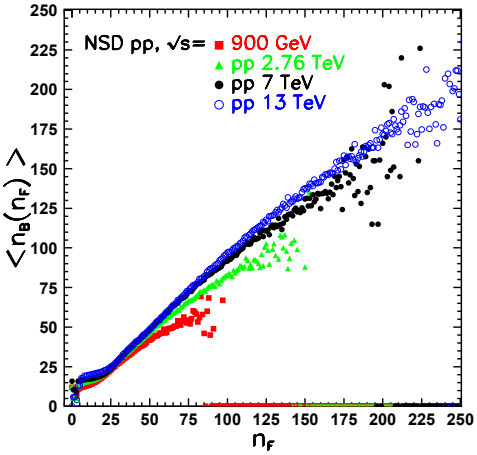

Figure 7. Forward-backward multiplicity correlations in NSD pp collisions at $\sqrt{s}$ = 0.9, 2.76, 7, and 13 TeV.

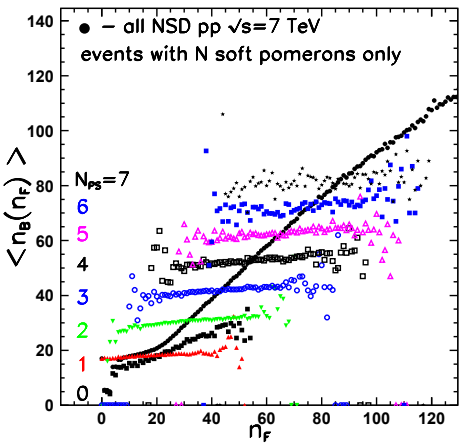

Figure 8. Dependence of average multiplicity $\langle n_B \rangle$ on n_F (solid circles) in NSD pp collisions at $\sqrt{s}$ = 7 TeV in QGSM. Curves indicate $\langle n_B(n_F) \rangle$ distributions for sub-events with only soft Pomerons, $N_{s\_Pom} = 0, 1, \ldots, 7$.

Figure 8 displays the $\langle n_B \rangle (n_F)$ dependencies calculated in QGSM for pp events at $\sqrt{s}$ = 7 TeV which proceed only via the soft Pomeron exchanges. The FB correlations for the sub-processes with fixed amount of soft Pomerons, varying from 1 to 7, are also plotted in Fig. 8. It is worth noting that FB correlations within each of the selected sample of events have zero slope, although the charged particle multiplicity measured on event-by-event basis changes from few hadrons up to one hundred. Not all topologies contribute to event with very small and very big multiplicity. This circumstance leads to reduction of the correlation strength in both multiplicity intervals.

At LHC energies the FB correlations in pp interactions were studied by the ALICE [21] and ATLAS [22] Collaborations. The analysis is performed in terms of gaps in pseudorapidity, η_{gap}, between the hadrons in forward and backward hemispheres, and widths of pseudorapidity bins, $\delta\eta$. Figure 9 presents the comparison of model calculations of the b_{corr} as a function of $\delta\eta$ at zero rapidity gap with the ALICE data for $\sqrt{s}$ = 900 GeV, 2.76 TeV and 7 TeV. The slope b_{corr} increases with broadening of $\delta\eta$ for all three energies. Note, that the strength of FB correlations drops with rising midrapidity gap [19].

ALICE Collaboration has also studied the FB correlations between different azimuthal sectors. Parameters of the study are as follows. The azimuthal angle of the sectors is $\varphi = \pi/4$ and the width of the bin is $\delta\eta = 0.2$. The data obtained for pp interactions at 900 GeV and 7 TeV are shown in Fig. 10 in comparison with the QGSM calculations. The correlations at $\sqrt{s}$ = 7 TeV are twice stronger than that at 900 GeV; other characteristics are pretty similar.

4 Conclusions

We apply the quark-gluon string model, based on Reggeon Field Theory, for the description of forward-backward multiplicity correlations in proton-proton collisions at ultrarelativistic energies. It

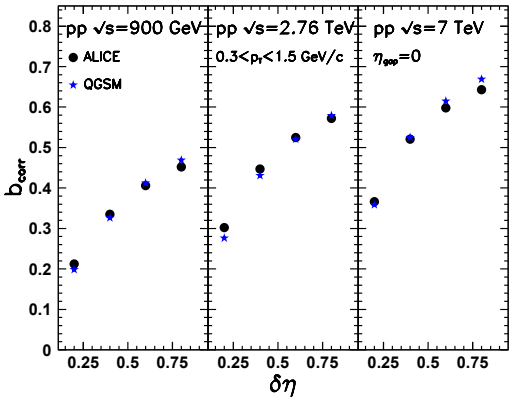

Figure 9. FB correlation parameter b_{corr} at $\eta_{gap} = 0$ in four rapidity bins: $\delta\eta = 0.2, 0.4, 0.6, 0.8$ in pp collisions at $\sqrt{s}$ = 900 GeV, 2.76 TeV, 7 TeV and 13 TeV. Stars and circles denote the model calculations and the ALICE data from [21], respectively.

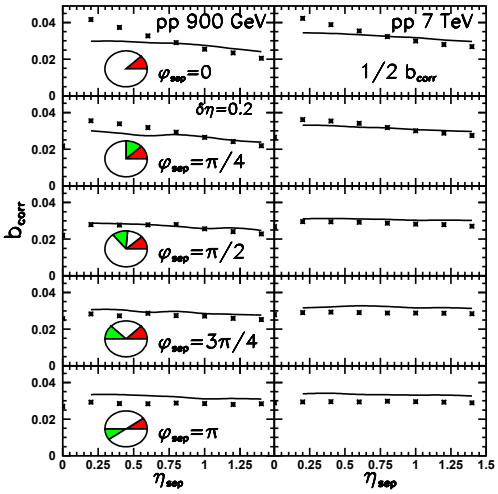

Figure 10. FB correlation parameter b_{corr} for azimuthally separated sectors of $\varphi = \pi/4$ as a function of midrapidity gap at fixed $\delta\eta = 0.2$ in pp collisions at $\sqrt{s}$ = 900 GeV (left) and 7 TeV (right). Results for 7 TeV are reduced by factor 2. Lines and asterisks denote the model calculations and the data from [21], respectively.

is shown that positive FB correlations arise in QGSM because of addition of different sub-processes with different mean multiplicities. For the individual sub-processes, their $\langle n_B \rangle (n_F)$ distributions are remarkably flat, although the event-by-event multiplicity can vary from few particles up to more than one hundred.

At c.m. energies about 10 GeV the number of diagrams describing $\bar{p}p$ collisions is larger than that for pp interactions. Therefore, FB correlations are stronger in $\bar{p}p$ case. At c.m. energies higher than 100 GeV the sets of diagrams for $\bar{p}p$ and pp collisions are similar. The further rise of the correlation strength occurs due to increasing number of soft and hard Pomerons allowed for a single event.

The correlation dependence is linear, $\langle n_B \rangle (n_F) = a + b_{corr} n_F$, for $\bar{p}p$ and pp collisions at all energies in question. However, for low and for very high multiplicities n_F the slopes b_{corr} are not so steep. Finally, the FB correlations take place mainly in the region $|x_F| < 0.1$, whereas for $|x_F| > 0.1$ the correlations are almost absent.

Acknowledgements

Fruitful discussions with M. Bleicher, L. Csernai and V. Vechernin are gratefully acknowledged. L.B. acknowledges financial support of the Alexander von Humboldt Foundation. J.B. thanks the German Research Foundation (DFG) for the financial support through the Project BL 1286/2-1.

References

[1] S. Uhlig, I. Derado, R. Meinke, H. Preissner, Nucl. Phys. B **132**, 15 (1978)

[2] K. Alpgaard *et al.*, UA5 Collab., Phys. Lett. B **123**, 361(1983)
[3] G.G. Alner *et al.*, UA5 Collab., Phys. Rep. **154**, 247 (1987)
[4] T.T. Chou, C.N. Yang, Phys. Lett. B **135**, 175 (1984)
[5] A. Capella, A. Krzywicki, Phys. Rev. D **18**, 4120 (1978)
[6] A. Capella, J.Tran Thanh Van, Z. Phys. C **18**, 85 (1983)
[7] J. Dias de Deus, Phys. Lett. B **100**, 177 (1981)
[8] M.A. Braun, C. Pajares, V.V. Vechernin, Phys. Lett. B **493**, 54 (2000)
[9] E.G. Boos *et al.*, Phys. Scripta **15**, 305 (1977)
[10] L.V. Bravina *et al.*, Sov. J. Nucl. Phys. **50**, 245 (1989)
[11] R.E. Ansorge *et al.*, UA5 Collab., Z. Phys. C **37**, 191 (1988)
[12] T. Alexopoulos *et al.*, E735 Collab., Phys. Lett. B **353**, 155 (1995)
[13] W. Braunschweig *et al.*, TASSO Collab., Z. Phys. C **45**, 193 (1989)
[14] R. Akers *et al.*, OPAL Collab., Phys. Lett. B **320**, 417 (1994)
[15] A.B. Kaidalov, Phys. Lett. B **116**, 459 (1982);
A.B. Kaidalov and K.A. Ter-Martirosyan, Phys. Lett. B **117**, 247 (1982)
[16] N.S. Amelin, L.V. Bravina, Sov. J. Nucl. Phys. **51**, 133 (1990)
[17] J. Bleibel, L.V. Bravina, E.E. Zabrodin, Phys. Rev. D **93**, 114012 (2016)
[18] E.E. Zabrodin *et al.*, these Proceedings.
[19] L.V. Bravina, J. Bleibel, E.E. Zabrodin, Phys. Lett. B (submitted).
[20] G. J. Alner *et al.*, UA5 Collab., Phys. Rep. **154**, 247 (1987)
[21] J. Adam *et al.*, ALICE Collab., J. High Energy Phys. **JHEP05**, 097 (2015)
[22] G. Aad *et al.*, ATLAS Collab., J. High Energy Phys. **JHEP07**, 019 (2012)